Journal of Solid State Chemistry 181 (2008) 1628–1633

Contents lists available at ScienceDirect

Journal of Solid State Chemistry

journal homepage: www.elsevier.com/locate/jssc

Alkyl-terminated crystalline Ge nanoparticles prepared from NaGe: Synthesis, functionalization and optical properties

Xuchu Ma, Fengyi Wu, Susan M. Kauzlarich *

Department of Chemistry, University of California at Davis, One Shields Avenue, Davis, CA 95616, USA

ARTICLE INFO

Article history:
Received 10 May 2008
Received in revised form
9 June 2008
Accepted 11 June 2008
Available online 13 June 2008

Keywords:
Zintl salt NaGe
Ge nanoparticles
Functionalization
Photoluminescence

ABSTRACT

High purity NaGe was directly prepared by a low-temperature reaction of NaH and Ge. The product was characterized by powder X-ray diffraction (XRD), scanning electron microscopy (SEM), and energy-dispersive X-ray (EDX) spectroscopy. This material is a useful starting reagent for the preparation of Ge nanoparticles. Hydrogen-terminated germanium (Ge) nanoparticles were prepared by reaction of NaGe with NH_4Br. These Ge nanoparticles could be prepared as amorphous or crystalline nanoparticles in quantitative yields and with a narrow size distribution. The nanoparticles were functionalized via thermally initiated hydrogermylation with 1-eicosyne, $CH_3(CH_2)_{17}C{\equiv}CH$ to produce alkyl-terminated Ge nanoparticles. The modified Ge nanoparticles were characterized by powder XRD, transmission electron microscopy (TEM), Fourier transform infrared (FT-IR) and Raman spectroscopy, and photoluminescence (PL) spectroscopy. The alkyl-functionalized Ge nanoparticles can be expected to have promising applications in many technological and biological areas.

1. Introduction

Group 14 semiconductor nanoparticles have useful applications in many areas of technology and biology. Silicon in nanoform, for example, has shown enhanced photovoltaic effects [1], and thermoelectric effects [2,3]. While there has been intense interest in solution synthesis of Si nanoparticles [4], Ge nanoparticles have received significantly less attention, perhaps due to controversy over the origin of light emission from small, surface passivated nanoparticles [5]. However, Ge nanoparticles have many applications also, such as precursors for thin film formation [6–8], for porous germanium (Ge) [9], and, regardless of the origin of light emission, for bioprobes [10,11].

Recently, Ge nanoparticles have been prepared via solution routes by a number of approaches, such as metathesis of Ge Zintl salts with $GeCl_4$ [12–14], supercritical thermolysis [15,16], reduction of Ge(II) [17] and Ge(IV) precursors [18–22], and thermal decomposition of organogermanes [22–25]. Though great progress has been made in recent years, the synthesis of Ge nanoparticles via solution routes remains an intense area of research [26]. In recent years, the focus has been on the synthesis of gram quantities of Ge nanoparticles [27], control of size [21,28], and the functionalization of their surface [29,30].

In this paper, we report the synthesis of Ge nanoparticles from the reaction of Zintl salt, NaGe, with NH_4Br. We also present a new, simple synthetic route to NaGe from the reaction of NaH with Ge powder that does not involve the use of niobium or tantalum tubing. The reaction of a metal silicide with NH_4Br has been shown to be successful in synthesizing hydrogen-terminated Si nanoparticles [31,32] and we have extended this route to produce hydrogen-terminated Ge nanoparticles. This is a simple oxidation–reduction route that provides gram quantities of high purity Ge nanoparticles with hydrogen on the surface. The resulting nanoparticles can be easily reacted with alkenes or alkynes via a hydrogermylation reaction [33] to produce alkyl bonded, functionalized nanoparticles.

2. Experimental section

2.1. Materials

Sodium hydride powder (NaH, 95%, Sigma-Aldrich), Ge powder (Ge, ⩾99%, Sigma-Aldrich), and 1-eicosyne (94%, GFS) were used as purchased without further treatment. Ammonium bromide (NH_4Br, ⩾99.99%, Sigma-Aldrich) was dried under dynamic vacuum at 100 °C for 12 h prior to usage. Diethylene glycol dibutyl ether (⩾98%, Sigma-Aldrich) was degassed before using. Glassware was dried overnight at 120 °C and transferred hot into an N_2-filled glove box. Unless otherwise stated, all samples are oxygen-sensitive and precautions must be taken to avoid exposure to

* Corresponding author. Fax: +1 530 752 8995.
E-mail address: smkauzlarich@ucdavis.edu (S.M. Kauzlarich).

0022-4596/$ - see front matter © 2008 Elsevier Inc. All rights reserved.
doi:10.1016/j.jssc.2008.06.018

oxygen. All manipulations were carried out under dry N_2 or Ar gas ($\geqslant$99% purity), in either a glove box filled with N_2 or on a standard Schlenk line, using standard anaerobic and anhydrous techniques.

NaGe was prepared from NaH and Ge powder. The pre-milled mixture of NaH and Ge (molar ratio of 1.2:1) was placed into an alumina crucible with an alumina cover in a quartz tube, and then heated at 270 °C for 3 h under flowing argon.

2.2. Preparation of crystalline (**1**) or amorphous (**2**) hydrogen-terminated germanium nanoparticles

Hydrogen-terminated crystalline Ge nanoparticles were synthesized by a solid-state process (**1**) or a solution process (**2**).

(**1**) *Solid-state process*: NaGe (0.1912 g, 2 mmol) and NH_4Br (0.3916 g, 4 mmol) were mixed in a glove box and placed into an alumina crucible, which was then placed in a one end sealed quartz tube with stopcock at the other end. The quartz tube was seated in a horizontal tube furnace under flowing of argon and heated at 300 °C for 12 h. This reaction produced hydrogen-terminated crystalline Ge nanoparticles and NaBr.

(**2**) *Solution process*: NaGe (0.1912 g, 2 mmol) and NH_4Br (0.3916 g, 4 mmol) were added to a Schlenk flask in the glove box. Degassed diethylene glycol dibutyl ether (80 mL) was added via a cannula to the flask and heated at 250 °C for 12 h under vacuum.

2.3. Synthesis of alkyl-terminated germanium nanoparticles

The product from process (**1**) was mixed with degassed diethylene glycol dibutyl ether (80 mL) in a Schlenk flask. 1.5 g of 1-eicosyne was added and the reaction mixture was heated at 250 °C for 12 h. The mixture was allowed to cool to room temperature resulting in a black solid with a yellow solution. The yellow solution was transferred via cannula to another Schlenk flask and vacuum-dried; a viscous orange oil was obtained. The black solid was collected and washed with excessive amounts of hexane, alcohol and distilled water successively to remove unreacted 1-eicosyne and NaBr, and then dried *en vacuo*.

After the reaction mixture of process (**2**) was cooled down to room temperature, 1.5 g of 1-eicosyne was added and heated at 250 °C for 12 h while stirring. This mixture was allowed to cool to room temperature and a black solid remained along with a yellow solution. The yellow solution was transferred via cannula to another Schlenk flask and vacuum-dried; a viscous orange oil was obtained. The black solid was collected and washed with excessive amounts of hexane, alcohol and distilled water to remove unreacted 1-eicosyne and NaBr and then dried *en vacuo*.

2.4. Characterization

Powder X-ray diffraction (XRD) data were collected on an INEL CPS 120 diffractometer with Co radiation ($\lambda = 1.78897$ Å) for NaGe (using an air sensitive holder) and Bruker D8 Advance X-ray diffractometer with Cu$K\alpha$ radiation ($\lambda = 1.54178$ Å) for Ge nanoparticles that are the solid phase obtained from these reactions. Raman spectra were obtained with a Renishaw RM1000 Research Laser Raman Microscope and an Argon laser operating at an excitation line of 514 nm for the Ge nanoparticles that are the solid phase obtained from these reactions. Transmission electron microscopy (TEM) was performed on a Philips CM-12, operating at 80 kV. Hitachi S-800T scanning electron microscopes (SEM) and an Oxford INCA energy-dispersive X-ray (EDX) spectrometer were employed to analyze chemical composition, with the accelerating voltage of 20 kV. SEM and EDX sample was prepared by standard techniques where grain dispersions were supported on double-sided carbon tape on specimen holders. The specimen holders were kept in a N_2-filled jar in a glove box and quickly transferred to the SEM instrument. The time for exposing to air was less than 3 s. TEM samples were prepared by dipping holey-carbon-coated, 400-mesh electron microscope grids into the hexane colloid solution and drying them at 120 °C overnight. Fourier transform infrared (FT-IR) spectroscopic data of the oily phase were obtained using a Shimadzu IR Prestige 21 equipped with a diffuse reflectance accessory. Photoluminescence (PL) spectra of the oily phase containing the Ge nanoparticles were measured on a FluoroMax-3P fluorometer, where the Ge nanoparticles were dispersed in hexane.

3. Results and discussion

The composition and morphology of NaGe was determined by XRD analysis, SEM, and EDX, as shown in Fig. 1. Fig. 1a shows a XRD pattern of the obtained NaGe (upper curve), which matches well with that of theoretical NaGe powder (lower curve)

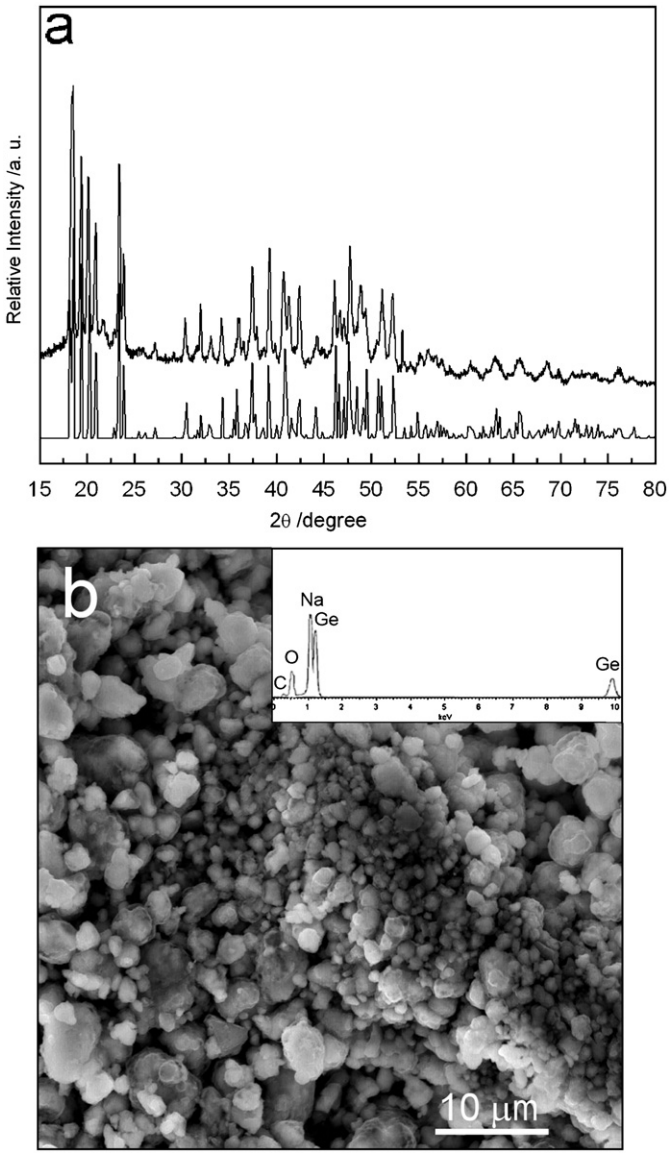

Fig. 1. (a) XRD patterns of NaGe: prepared from optimized reactions of NaH with Ge (upper curve) and calculated from single-crystal X-ray diffraction data (lower curve), and (b) SEM image of NaGe and the inset is an EDX spectrum.

calculated from single-crystal XRD data [34]. Lattice parameters obtained from the powder XRD data of the as-prepared product are $a = 12.327 \pm 0.005$ Å, $b = 6.705 \pm 0.002$ Å, $c = 11.417 \pm 0.004$ Å, and $\beta = 120.00 \pm 0.04^\circ$, consistent with the published parameters of NaGe ($a = 12.33$ Å, $b = 6.70$ Å, $c = 11.42$ Å, and $\beta = 120.0^\circ$). Two small peaks at 21.8° and 53.2° in Fig. 1a are belonging to the air sensitive holder used to obtain the data. Fig. 1b is a SEM image of the resulting NaGe, indicating that the diameter of NaGe particles is in the range of 1.5–3 μm. An EDX spectrum of the products obtained from optimized reactions of NaH with Ge is shown in inset of Fig. 1b. From inset of Fig. 1b, Na and Ge elements are detected and atomic ratio of Na:Ge is 1:1.05, consistent with the stoichiometric formula of NaGe. The carbon (C) signal comes from the carbon tape (support), while the oxygen (O) signal most likely originates from oxidization of the sample surface that may occur during the sample transfer from the glove box to SEM instrument. No N or Br peaks can be found in the EDX spectrum, indicating that the as-prepared product is composed of pure NaGe.

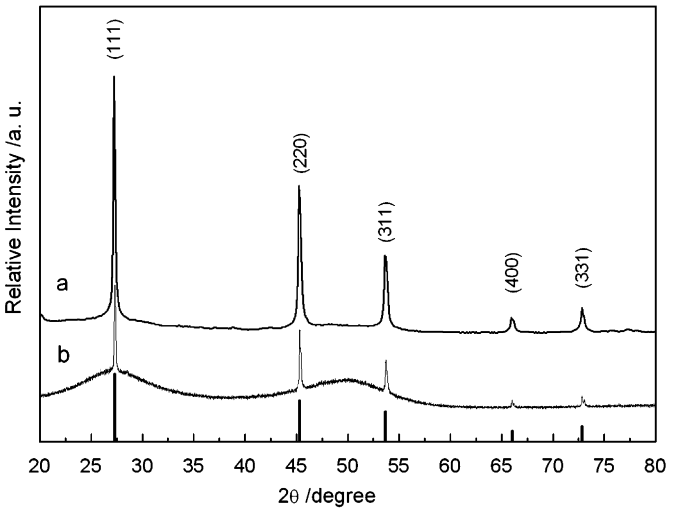

Fig. 2. XRD patterns of Ge nanoparticles obtained by: (a) process (**1**) (upper curve) and (b) process (**2**) (middle curve). Calculated peaks with indices for crystalline Ge are provided.

NaGe is reacted with NH_4Br to produce hydrogen-terminated Ge nanoparticles according to the reaction:

$$NaGe + NH_4Br \rightarrow Ge)-H + NH_3 + NaBr$$

where Ge)–H represents hydrogen-terminated Ge nanoparticles. The hydrogen-terminated Ge material is stable in air for less than 1 h.

This reaction was run either under flowing argon at 300 °C (process (**1**)) or in diethylene glycol dibutyl ether at 250 °C (process (**2**)). Fig. 2a and b show powder XRD patterns of the solid phase products obtained from processes (**1**) and (**2**), respectively, after capping with 1-eicosyne. For products prepared from (**1**), five diffraction peaks at 27.3°, 45.3°, 53.8°, 66.1° and 73.0° correspond to the (111), (220), (311), (400) and (331) reflections of cubic-structure crystalline Ge (JCPDS files no. 04-0545, $a = 5.657$ Å). In Fig. 2b, the observation of two broad diffraction peaks at approximately 27.3° and 50.0° together with additional crystalline peaks suggests a mixture of amorphous and crystalline Ge [20,21]. It is noteworthy that no signals from Ge dioxide are observed in the XRD patterns, though the powders are washed with distilled water. This is assumed to be the case since the surfaces have been terminated with alkane and GeO_2 is water soluble. The yellow oily phase did not give rise to an observable powder diffraction, presumably because the nanoparticles were embedded in an organic matrix similar to what we have observed in reduction reactions to form Ge nanoparticles [21].

Morphology and size distribution of the alkyl-terminated Ge nanoparticles obtained from processes (**1**) and (**2**) were observed by TEM. The nanoparticles from the oily phase, as shown in Fig. 3, are isolated from each other and well-dispersed on the grid. Fig. 3a and b exhibit typical micrographs of alkyl-terminated crystalline and amorphous Ge nanoparticles, respectively. The size distribution for crystalline Ge nanoparticles is 4.0 ± 1.0 nm and

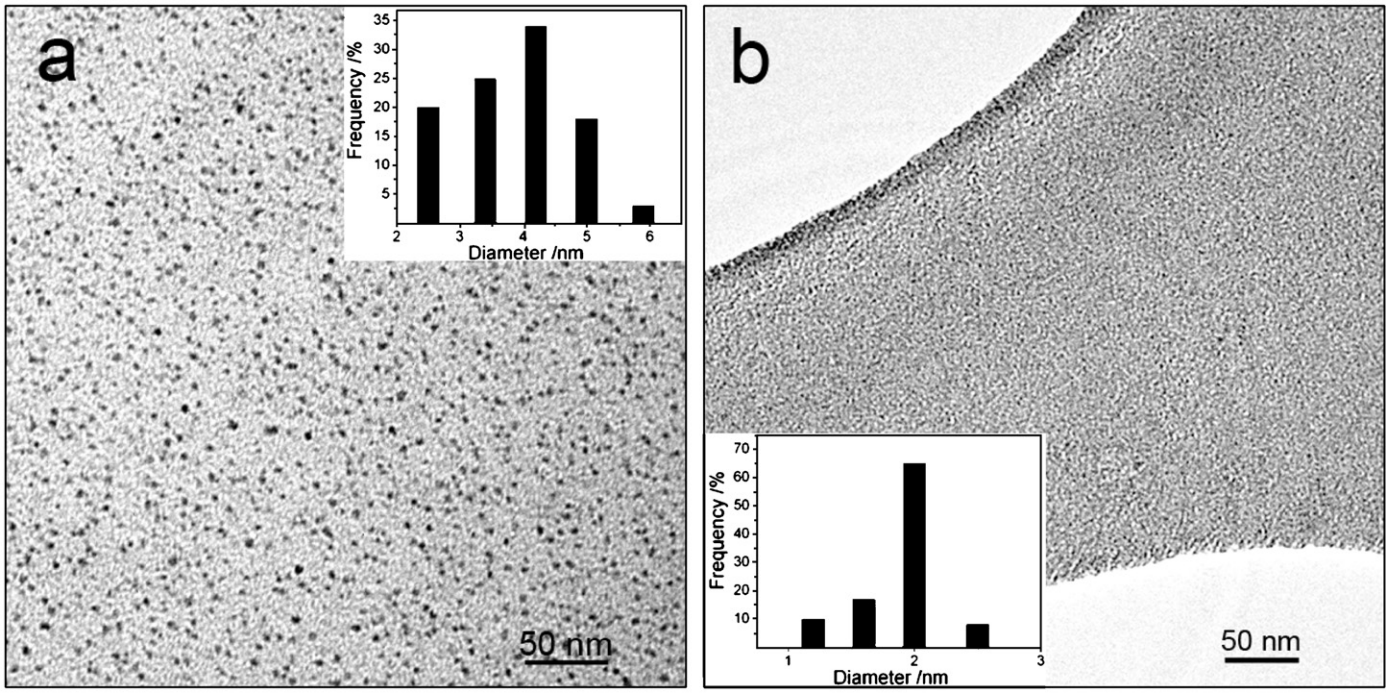

Fig. 3. TEM images and size distribution histograms of alkyl-terminated Ge nanoparticles: (a) crystalline and (b) amorphous.

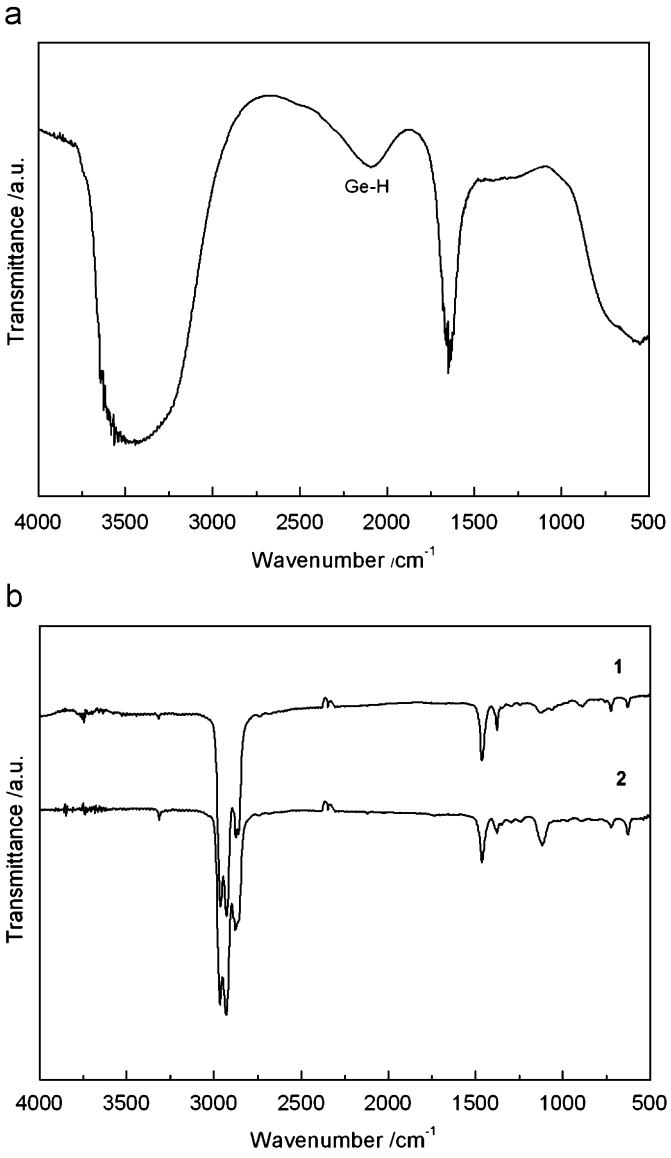

Fig. 4. FT-IR spectra of (a) hydrogen-terminated crystalline Ge and (b) alkyl-terminated Ge nanoparticles obtained from processes (**1**) and (**2**) and terminated via hydrogermylation, respectively.

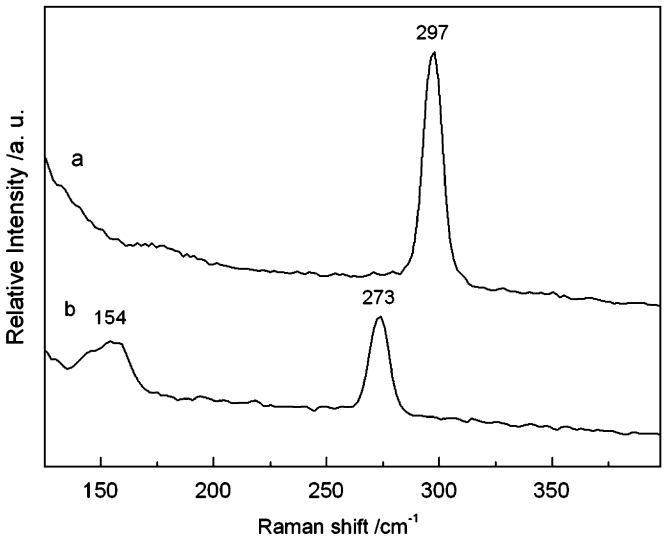

Fig. 5. Raman spectra of alkyl-terminated (a) crystalline and (b) amorphous Ge nanoparticles.

that for amorphous Ge nanoparticles is 1.9 ± 0.5 nm. Size distribution histograms of Ge nanoparticles are shown in Fig. 3a and b, and these are based on surveys of 500 particles from different regions of the TEM grids. No aggregation is observed.

Fig. 4a shows FT-IR spectrum of hydrogen-terminated crystalline Ge, and Fig. 4b presents those of alkyl-terminated crystalline and amorphous Ge nanoparticles from the oily phase obtained from process (**1**) and (**2**), respectively. The spectra of both samples correspond well with stretches expected for the organic groups. The IR absorption spectrum of the hydrogen-terminated crystalline Ge, shown in Fig. 4a, exhibits the characteristic stretching vibration mode band ν(Ge–H) at 2100 cm^{-1} [33], and the other two peaks at 3500, and 1640 cm^{-1} correspond to N–H stretching and bending modes. The N–H modes may be due to the presence of NH_4Br, as this sample was not washed with water, but the solution of the mixture was drop dried on a KBr salt plate. The FT-IR spectra in Fig. 4b reveal three peaks at 2961, 2925, and 2872 cm^{-1} that correspond to C–H stretching modes for CH_2 and CH_3 groups, indicating the presence of hydrocarbon species. The peaks at 1464 and 1380 cm^{-1} are attributed to the symmetric and asymmetric bends of the methyl group, respectively. Although FT-IR spectroscopy does not provide definitive proof that organic ligands are bonded to the Ge nanoparticle surface, results from FT-IR spectra are consistent with the presence of a hydrocarbon layer on the particle surface [17].

Raman spectroscopy could be used to evaluate bonding in the Ge core by monitoring Ge–Ge optical phonon (OP) vibration [26]. Fig. 5 shows Raman spectra of the Ge nanoparticles that are the solid phase obtained from these reactions. Fig. 5a is a Raman spectrum of Ge nanoparticles obtained from process (**1**), where a peak positioned at ~297 cm^{-1} can be observed. According to the literature, this peak can be attributed to crystalline Ge where the Ge–Ge stretch is 302 cm^{-1} [26]. Fig. 5b is a Raman spectrum of Ge nanoparticles from process (**2**), showing two Raman shifts at about 154 and 273 cm^{-1}. These two Raman peaks are characteristic of amorphous Ge [35].

PL spectroscopy was used to investigate the optical properties of the Ge nanoparticles in the oily phase. Fig. 6a and b show the normalized PL spectrum of alkyl-terminated crystalline and amorphous Ge nanoparticles in hexane prepared from processes (**1**) and (**2**), respectively. Fig. 6a shows a series of intense luminescence peaks with a relatively narrow region from 368 to 415 nm, with excitation from 320 to 350 nm. The maximum intensity emission is centered at 368 nm with an excitation wavelength of 320 nm. A theoretical calculation shows that indirect band-gap energy (E_{gap}) of Ge nanocrystal is size-dependent and the calculated E_{gap} for ~5 nm Ge nanocrystals is about 2.1 eV [36,37]. This is not consistent with the observed PL excitation spectra in Fig. 6a. Therefore, as a possible explanation, we suggest that PL emission from Ge nanocrystallite positioned at ~400 nm might be due to two reasons: (1) vibrations of hydrocarbon layer absorbed on the surface of these synthesized Ge nanocrystals, (2) defects on surface of Ge nanocrystals [37]. Fig. 6b shows a series of intense luminescence peaks with a relatively narrow region from 411 to 438 nm, with excitation from 350 to 380 nm. The maximum intensity emission is centered at 423 nm with an excitation wavelength of 360 nm. Changes in the excitation wavelength excite different size populations of nanoparticles, resulting in the variation of emission wavelengths. Though some questions about the PL spectra remain, the larger increase in energy of the PL relative to band-gap of bulk Ge and monotonic shift in PL wavelength with excitation wavelength

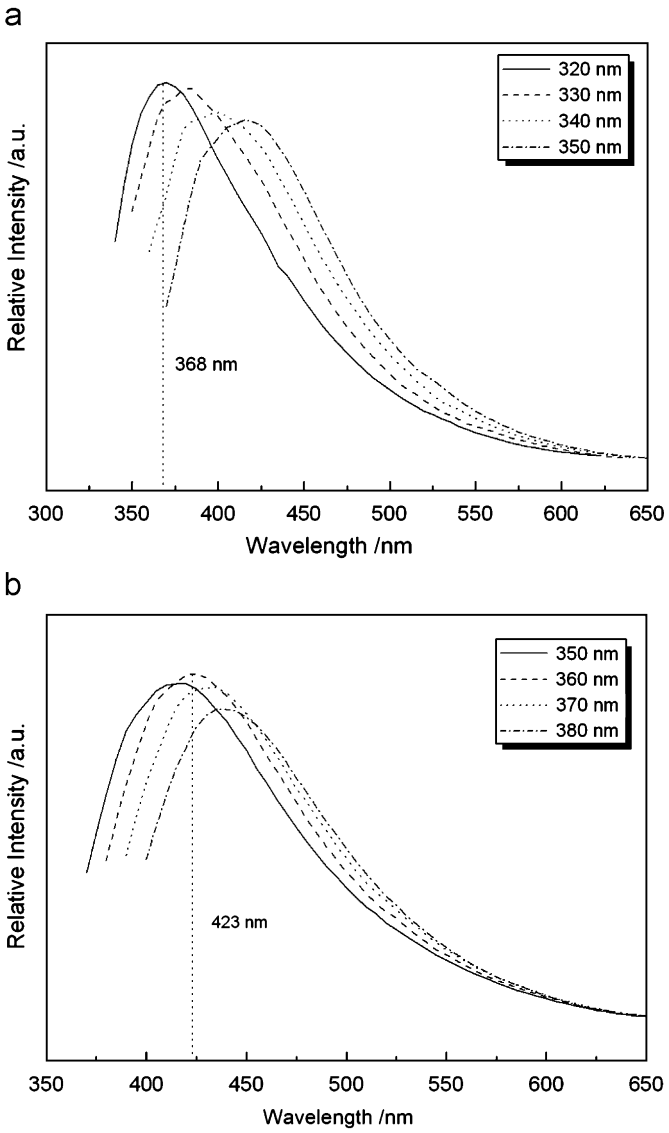

Fig. 6. Photoluminscence (PL) spectra of (a) crystalline and (b) amorphous Ge nanoparticles under different excitation wavelength dispersed in hexane.

point to quantum confinement as a contributing factor to such interesting PL behavior [38].

To understand the influence of reaction temperature and reaction time on crystallinity and size of Ge nanoparticles, a series of control experiments were performed under similar conditions. We find that, for process (**1**), Ge nanoparticles are converted from amorphous to a mixture of amorphous and crystalline when the reaction time is increased from 2 to 8 h. Ge nanocrystallites could be obtained when the reaction time reaches 12 h, as shown in Fig. 7. However, for process (**2**), the reaction temperature and time have no obvious effect on crystallinity and size of Ge nanoparticles and always exhibited a diffraction pattern similar to that shown in Fig. 2.

4. Conclusion

In summary, we have developed a simple route to produce alkyl-terminated Ge nanoparticles. Alkyl-terminated crystalline Ge nanoparticles can be obtained via an initial solid-state process (**1**) followed by thermal hydrogermylation in an organic solvent. Alkyl-terminated amorphous Ge nanoparticles can be synthesized

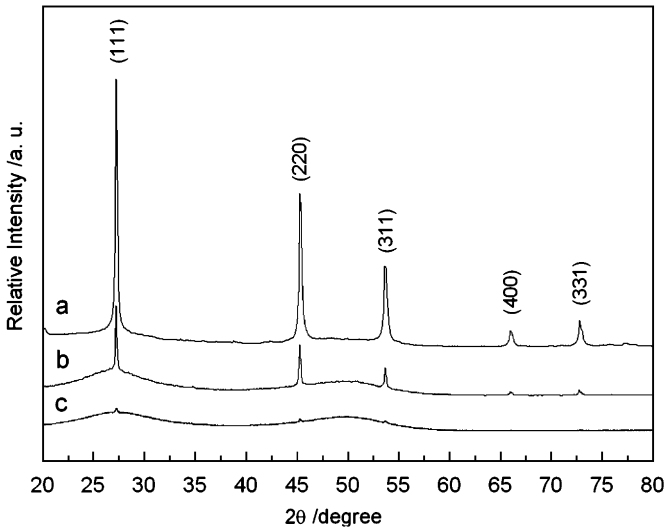

Fig. 7. XRD patterns of Ge nanoparticles from process (**1**) obtained at different times: (a) 12 h, (b) 8 h and (c) 2 h.

by a two-step refluxing process (**2**) and thermal hydrogermylation. The average size of Ge nanoparticles ranges from 1 to 5 nm with a narrow size distribution. Such alkyl-terminated Ge nanoparticles displayed strong PL in the blue region of the visible spectrum. The growth conditions of this new method can be further optimized for synthesis of crystalline nanoparticles.

Acknowledgment

We thank NSF (DMR-0600742) and Nanohmics, Inc. for funding.

References

[1] M. Stupca, M. Alsalhi, T. Al Saud, A. Almuhanna, M.H. Nayfeh, Appl. Phys. Lett. 91 (2007) 063107.
[2] A.I. Hochbaum, R.K. Chen, R.D. Delgado, W.J. Liang, E.C. Garnett, M. Najarian, A. Majumdar, P.D. Yang, Nature 451 (2008) U163–U165.
[3] A.I. Boukai, Y. Bunimovich, J. Tahir-Kheli, J.K. Yu, W.A. Goddard, J.R. Heath, Nature 451 (2008) 168–171.
[4] J.G.C. Veinot, Chem. Commun. (2006) 4160–4168.
[5] D. Gerion, N. Zaitseva, C. Saw, M.F. Casula, S. Fakra, T. Van Buuren, G. Galli, Nano Lett. 4 (2004) 597–602.
[6] H.W. Chiu, S.M. Kauzlarich, E. Sutter, Langmuir 22 (2006) 5455–5458.
[7] A. Watanabe, M. Unno, F. Hojo, T. Miwa, J. Mater. Sci. Lett. 20 (2001) 491–493.
[8] E.V. Johnson, G. Patriarche, P.R.I. Cabarrocas, Appl. Phys. Lett. 92 (2008) 103–108.
[9] J. Shieh, H.L. Chen, T.S. Ko, H.C. Cheng, T.C. Chu, Adv. Mater. 16 (2004) 1121–1124.
[10] T.N. Lambert, N.L. Andrews, H. Gerung, T.J. Boyle, J.M. Oliver, B.S. Wilson, S.M. Han, Small 3 (2007) 691–699.
[11] B.A. Hernandez-Sanchez, T.J. Boyle, T.N. Lambert, S.D. Daniel-Taylor, J.M. Oliver, B.S. Wilson, D.S. Lidke, N.L. Andrews, IEEE Trans. Nanobiosci. 5 (2006) 222–230.
[12] B.R. Taylor, S.M. Kauzlarich, G.R. Delgado, H.W.H. Lee, Chem. Mater. 11 (1999) 2493–2500.
[13] C.S. Yang, S.M. Kauzlarich, Y.C. Wang, Chem. Mater. 11 (1999) 3666–3670.
[14] B.R. Taylor, S.M. Kauzlarich, H.W.H. Lee, G.R. Delgado, Chem. Mater. 10 (1998) 22–24.
[15] X.M. Lu, B.A. Korgel, K.P. Johnston, Nanotechnology 16 (2005) S389–S394.
[16] X.M. Lu, K.J. Ziegler, A. Ghezelbash, K.P. Johnston, B.A. Korgel, Nano Lett. 4 (2004) 969–974.
[17] X.M. Lu, B.A. Korgel, K.P. Johnston, Chem. Mater. 17 (2005) 6479–6485.
[18] A. Kornowski, M. Giersig, R. Vogel, A. Chemseddine, H. Weller, Adv. Mater. 5 (1993) 634–636.
[19] J.R. Heath, J.J. Shiang, A.P. Alivisatos, J. Chem. Phys. 101 (1994) 1607–1615.
[20] H.W. Chiu, C.N. Chervin, S.M. Kauzlarich, Chem. Mater. 17 (2005) 4858–4864.
[21] H.W. Chiu, S.M. Kauzlarich, Chem. Mater. 18 (2006) 1023–1028.
[22] J.H. Warner, R.D. Tilley, Nanotechnology 17 (2006) 3745–3749.

[23] H. Gerung, S.D. Bunge, T.J. Boyle, C.J. Brinker, S.M. Han, Chem. Commun. (2005) 1914–1916.
[24] H. Gerung, T.J. Boyle, L.J. Tribby, S.D. Bunge, C.J. Brinker, S.M. Han, J. Am. Chem. Soc. 128 (2006) 5244–5250.
[25] J.H. Warner, Nanotechnology 17 (2006) 5613–5619.
[26] E.J. Henderson, C.M. Hessel, J.G.C. Veinot, J. Am. Chem. Soc. 130 (2008) 3624–3632.
[27] W.Z. Wang, B. Poudel, J.Y. Huang, D.Z. Wang, S. Kunwar, Z.F. Ren, Nanotechnology 16 (2005) 1126–1129.
[28] J.P. Wilcoxon, P.P. Provencio, G.A. Samara, Phys. Rev. B 64 (2001).
[29] R.S. Tanke, S.M. Kauzlarich, T.E. Patten, K.A. Pettigrew, D.L. Murphy, M.E. Thompson, H.W.H. Lee, Chem. Mater. 15 (2003) 1682–1689.
[30] E. Fok, M.L. Shih, A. Meldrum, J.G.C. Veinot, Chem. Commun. (2004) 386–387.
[31] D. Neiner, H.W. Chiu, S.M. Kauzlarich, J. Am. Chem. Soc. 128 (2006) 11016–11017.
[32] X. Zhang, D. Neiner, S. Wang, A.Y. Louie, S.M. Kauzlarich, Nanotechnology 18 (2007) 095601–095606.
[33] J.M. Buriak, Chem. Rev. 102 (2002) 1272–1308.
[34] R. Schäfer, W. Klemm, Z. Anorg. Allg. Chem. 312 (1961) 214–220.
[35] A. Kailer, K.G. Nickel, Y.G. Gogotsi, J. Raman Spectrosc. 30 (1999) 939–947.
[36] T. Takagahara, K. Takeda, Phys. Rev. B 46 (1992) 15578–15581.
[37] H.P. Wu, M.Y. Ge, C.W. Yao, Y.W. Wang, Y.W. Zeng, L.N. Wang, G.Q. Zhang, J.Z. Jiang, Nanotechnology 17 (2006) 5339–5343.
[38] B.R. Taylor, G.A. Fox, L.J. Hope-Weeks, R.S. Maxwell, S.M. Kauzlarich, H.W.H. Lee, Mater. Sci. Eng. B-Solid 96 (2002) 90–93.